Reliability Analysis of the Integrated Navigation System Based on Real Trajectory and Calculation of Safety Margin Between Trains

SEONG YUN CHO[1], MYEONG SEOK CHAE[2], AND KYUNG HO SHIN[3]

[1]Department of Robotics and Mobility, Kyungil University, Gyeongsan 38428, South Korea
[2]Department of IT Engineering, Kyungil University, Gyeongsan 38428, South Korea
[3]Northern Railroad Research Division, Korea Railroad Research Institute, Uiwang 16105, South Korea

Corresponding author: Kyung Ho Shin (khshin@krri.re.kr)

ABSTRACT A safety margin must always be maintained between trains. To this end, position data of all trains must be provided to the railway system in real time. Basically, this data has been provided based on the infrastructure installed on the railway. However, enormous costs are required to install the infrastructure, and continuous maintenance is required. In addition, cases of accidents due to un-detection or false-detection of trains are being reported as news. Due to these problems, researches on infra-less navigation system for trains have been conducted. Taking into account the blocking phenomenon of Global Positioning System (GPS)/Global Navigation Satellite System (GNSS) signals in tunnels, the navigation system for trains should constitute an integrated navigation system. However, the accuracy and reliability of navigation solution provided by the integrated navigation system are not always satisfied. And this can lead to instability of the railway system. Therefore, the navigation solution for trains must have high accuracy and also the reliability information of the corresponding navigation solution must be provided. In this article, we construct an Inertial Navigation System (INS)/GPS/Non-Holonomic Constraints (NHC) integrated navigation system for trains with NHC motion. A simulation trajectory is generated considering the real trajectory, and the accuracy and reliability of the navigation information according to the trajectory and measurements are analyzed together. And based on this information, we propose a method to calculate the safety margin between trains. The performance of the proposed technology is verified through a real trajectory-based Monte Carlo simulation.

INDEX TERMS Integrated navigation system, reliability analysis, safety margin, train navigation.

I. INTRODUCTION

Navigation information including the position of a moving object is necessary for guidance/control to move to a destination, and also to provide information for safety and convenience purpose [1], [2]. Until now, the position information of trains has been provided to maintain the safety margin between trains and schedule-based operation of trains in the railway system. The position information of trains are generally obtained by detecting the trains based on infrastructure installed on the railroad such as Balise and track circuits. This system has high accuracy and reliability of train detection [3], [4]. However, infrastructure must be installed at regular

The associate editor coordinating the review of this manuscript and approving it for publication was Cristian Zambelli[iD].

intervals across the entire railroad, and reliability must be maintained through periodic maintenance. For this, a large cost is required, and the consumption of manpower and time is essential. In addition, there are cases in which accidents were caused by the infrastructure not being able to detect trains or by making false detections. Motivated by these reasons, we are researching a technology for a train navigation system based on a sensor system mounted on a train instead of infrastructure [5]–[8].

Global Positioning System (GPS)/Global Navigation Satellite System (GNSS) is the most commonly used navigation system [9]. In an open sky environment, the satellite navigation provides not only the exact position information of fast-moving trains, but also velocity and heading information [10]. However, satellite signals cannot be used or

distorted in tunnels, mountains and urban areas, and their use is limited [4]–[6]. For availability and accuracy, an integrated navigation using Dead Reckoning (DR) or Inertial Navigation System (INS) with GPS can be considered. DR is a navigation technology that uses a speedometer and a geomagnetic sensor. Since trains slip a lot on the railroad in the acceleration/deceleration sections, the error in DR using a speedometer mounted on wheels is bounded to be large [13]. To solve this problem, map matching is sometimes used together [5], [15], [16]. Considering this problem, this article deals with a system integrating INS and GPS. The INS is not affected by the slip of the train by using a non-contact inertial sensors. However, INS-based navigation information has an error that accumulates over time due to the errors included in the sensor output and the initial errors [13], [17]. This error can be compensated through integration with GPS [19]. However, in places where GPS signals cannot be received or GPS signals are distorted, such as in tunnels, it is difficult to correct INS error through GPS data, or rather, INS errors may be increased through incorrect error correction. In this case, therefore, the INS alone calculates the navigation solution, and the INS error increases. Therefore, we deal with the INS/GPS/Non-Holonomic Constraints (NHC) integrated navigation system considering the NHC movement of trains [20], [21].

In this article, a method of calculating the safety margin between trains based on the navigation information provided by the integrated navigation system is studied. The accuracy of the navigation solution is important. As well as this, however, the reliability information of the navigation solution is also very important because the use of solution with low reliability may be restricted. In this article, the reliability of the navigation solution of the integrated navigation system is calculated through the error covariance matrix. However, this information does not always reflect the accurate reliability of the navigation solution. That is, there may be a case where the error covariance of the integration filter and the Root mean Squared Errors (RMSE) calculated through Monte Carlo simulation do not match [22].

Motivated by the problems of the safety margin between trains based on the integrated navigation system, and the reliability of the integrated navigation system, the following researches were conducted in this article. First, the reliability of the state error covariance matrix of the navigation filter is analyzed according to the use of NHC information through simulation. And based on this, it shows that the use of GPS measurement and NHC information together allows the navigation system to provide higher accuracy and reliability. The trajectory for the simulation is created based on the real trajectory of the test bed site. The reason is to show the suitability of the simulation-based research conducted in this article instead of the experiment-based research, and also to analyze in advance the results that can be obtained when applying the navigation system to be developed based on this research in the field. To this end, a reference trajectory is created by adding simulation conditions to the position data

obtained through an actual driving test. Then, sensor data is generated based on the reference trajectory. After verifying the accuracy of the generated sensor data, it is used as sensor data for simulation.

Then, we propose a method to calculate the safety margin between trains using the navigation solution with accuracy and reliability. The safety margin is calculated by using the position and velocity solution provided by the integrated navigation system and the reliability information of these information together. In addition, it is verified based on simulation that the braking alarm is properly provided to subsequent train to maintain a certain safety distance. Through this, it is confirmed that even when there is no infrastructure on the railroad, the safety margin between trains is accurately calculated through the navigation system installed on the trains, and based on this, it is possible to operate the railroad system that guarantees safety.

The rest of this article is organized as follows. Section II describes the technique of generating reference trajectory and sensor data based on real trajectory, and Section III designs INS/GPS/NHC integrated navigation system based on Cubature Kalman Filter (CKF) and generates reliability information of the navigation solution. Section IV, a technique to calculate the safety margin between trains based on the navigation solution is proposed, and the simulation-based performance analysis is performed in Section V. And the final section concludes.

II. SENSOR DATA GENERATION FOR SIMULATION BASED ON REAL TRAJECTORY

In order to simulate the performance analysis of the navigation system, a trajectory must be created first, and sensor data to perform navigation on the trajectory must be generated. In this study, the simulation trajectory is generated based on the real railroad trajectory selected as a testbed, not the virtual trajectory. To this end, in this section, a reference trajectory is generated using the position data acquired through the actual vehicle test. Then, IMU and GPS data are generated based on the reference trajectory.

A. REFERENCE TRAJECTORY GENERATION

A precise navigation system was mounted on the train and the track information was acquired while the train was operated on the real trajectory selected as the testbed. However, this data has been obtained regardless of the conditions required for the simulation. So, the position data is newly created by fusing this data with the simulation conditions. This position data is referred to as a reference trajectory in this article, and the simulation conditions include acceleration, deceleration, maximum speed, and sensor output frequency.

The movement of the train can be simplified with the NHC-based 4-degree of freedom movement. That is, it is possible to generate 3-dimensional position information of the train by using the forward direction speed and the 3-axis angular velocity. First, the navigation information is initialized as (1). The navigation information of the train consists of the

position and velocity information of the navigation system mounted on the locomotive with respect to the Earth, and the relative attitude information of the train's body coordinate frame with respect to the navigation coordinate frame. And the body coordinate frame is defined as a Cartesian coordinate system in which the x axis points along the train's forward longitudinal axis, the y axis out to the right direction, and the z axis points down [17].

$$\mathbf{Att}_0 = [\,\phi_0^A \quad \theta_0^A \quad \psi_0^A\,]^T$$
$$\mathbf{Vel}_0^n = [\,v_{N,0} \quad v_{E,0} \quad v_{D,0}\,]^T = \mathbf{C}_{b,0}^n[\,v_{x,0} \quad 0 \quad 0\,]^T$$
$$\mathbf{Pos}_0 = [\,Lat_0^A \quad Lon_0^A \quad Hgt_0^A\,]^T \tag{1}$$

where $\mathbf{Pos}_0$ and $\mathbf{Att}_0$ are the initial position (latitude, longitude, and height) and Euler angles (roll, pitch, and yaw) respectively acquired through the actual vehicle test, and $\mathbf{C}_{b,0}^n$ is the Direction Cosine Matrix (DCM) calculated using the Euler angles [17]. $\mathbf{Vel}_0^n$ is the velocity in the navigation coordinate frame, and $v_{x,0}$ is the speed in the forward direction of the train and is set to 0. The superscript A means acquisition through actual vehicle testing.

The position of the train is updated as follows using velocity information [13], [17].

$$\mathbf{Pos}_t = \mathbf{Pos}_{t-1} + \begin{bmatrix} v_{N,t-1}/(R_M + Hgt_{t-1}) \\ v_{E,t-1}/(R_T + Hgt_{t-1})\cos Lat_{t-1} \\ -v_{D,t-1} \end{bmatrix} \Delta t \tag{2}$$

where Δt is the speed update time interval, which is the same as the output period of the IMU. R_M and R_T are the Earth's radius calculated in the latitude and longitude directions, respectively, and are calculated as follows:

$$R_M = \frac{R_0(1-e^2)}{(1-e^2\sin^2 L)^{3/2}}, \quad R_T = \frac{R_0}{(1-e^2\sin^2 L)^{1/2}} \tag{3}$$

where $R_0 = 6,278,137m$ and $e = 0.0818191908426$ are the equatorial radius and eccentricity of the Earth's ellipsoid, respectively.

To update the position, the velocity must be updated. The train moves only in the forward direction on the railroad, and the forward speed can be updated as follows:

$$v_{x,t} = v_{x,t-1} + a_{x,t-1} \cdot \Delta t \tag{4}$$

where $a_{x,t-1}$ is the forward acceleration at time $t-1$. This acceleration value can be set based on the acceleration and deceleration conditions and the maximum speed of trains.

In order to update the velocity in the navigation coordinate frame, the attitude must be updated as follows:

$$\psi_t = \tan^{-1}\frac{(Lon_j^A - Lon_{k+1}^A)(R_T + Hgt_t)\cos Lat_t}{(Lat_j^A - Lat_{k+1}^A)(R_M + Hgt_t)} \tag{5}$$

$$\theta_t = \tan^{-1}\frac{Hgt_j^A - Hgt_{k+1}^A}{\sqrt{d_{Lat}^2 + d_{Lon}^2}} \tag{6}$$

$$\phi_t = (\phi_k^A + \phi_{k+1}^A)/2 \tag{7}$$
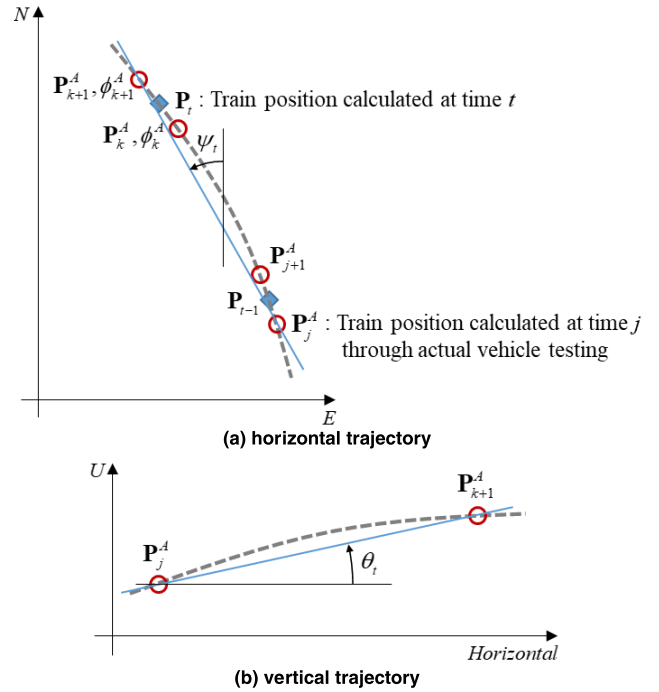

FIGURE 1. Conceptual diagram of data processing for generating a reference trajectory based on a real trajectory.

Figure 1 must first be explained to understand these equations. In this figure, the two positions continuously calculated through (2) and the measured position data close thereto are shown together. That is, the measured positions before and after the position calculated at time t are recognized as $\mathbf{Pos}_k^A$ and $\mathbf{Pos}_{k+1}^A$. When the measured position data is obtained in this way, the yaw and pitch angles at time t can be calculated through (5) and (6), respectively. That is, the attitude is updated using the measured position at $t = j$ and $t = k+1$. In (6), d is calculated as follows.

$$d_{Lat} = (Lat_j^A - Lat_{k+1}^A)(R_M + Hgt_t)$$
$$d_{Lon} = (Lon_j^A - Lon_{k+1}^A)(R_T + Hgt_t)\cos Lat_t \tag{8}$$

The yaw and pitch angles can be calculated using the continuously measured position information in a dynamic situation. However, it is difficult to calculate the roll angle using the location information. Since the rotation of the roll axis occurs in the rotation section of the train, the roll angle must be updated in consideration of the actual environment in order to reflect reality in the simulation. In this article, therefore, the roll angle is updated using the measured roll angles as in (7).

The DCM is calculated using the updated attitude, and then the velocity in the navigation coordinate frame is updated using the forward speed and the DCM based on (1) [13].

The position data generated by this method satisfies the simulation conditions and forms the same trajectory as the real railroad trajectory. This is determined as the reference trajectory for simulations.

B. SENSOR DATA GENERATION

IMU data can be generated based on the generated reference trajectory. For this, first, the velocity in the navigation coordinate frame is calculated through the position difference of the reference trajectory.

$$\mathbf{Vel}_t^n = \begin{bmatrix} (Lat_t^R - Lat_{t-1}^R)(R_M + Hgt_{t-1}^R) \\ (Lon_t^R - Lon_{t-1}^R)(R_T + Hgt_{t-1}^R)\cos Lat_{t-1}^R \\ Hgt_t^R - Hgt_{t-1}^R \end{bmatrix} / \Delta t \tag{9}$$

where the superscript R means the reference trajectory.

Attitude information can be obtained by time synchronization from the reference trajectory data and this information can be converted into DCM, and quaternion [18]. Based on this information, IMU data is created as follows:

$$\mathbf{f}_t^b = (\mathbf{C}_{b,t-1}^n)^T(d\mathbf{Vel}_t^n + 2\boldsymbol{\omega}_{ie,t-1}^n + \boldsymbol{\omega}_{en,t-1}^n - \mathbf{g}_{t-1}^n)$$
$$\boldsymbol{\omega}_{ib,t}^b = \boldsymbol{\omega}_{nb,t}^b + (\mathbf{C}_{b,t-1}^n)^T(\boldsymbol{\omega}_{ie,t-1}^n + \boldsymbol{\omega}_{en,t-1}^n) \tag{10}$$

where

$$d\mathbf{Vel}_t^n = (\mathbf{Vel}_t^n - \mathbf{Vel}_{t-1}^n)/\Delta t \tag{11}$$

$$\boldsymbol{\omega}_{ie,t-1}^n = \begin{bmatrix} \Omega_{ie}\cos Lat_{t-1} & 0 & -\Omega_{ie}\sin Lat_{t-1} \end{bmatrix}^T \tag{12}$$

$$\boldsymbol{\omega}_{en,t-1}^n = \begin{bmatrix} \dot{Lon}_{t-1}\cos Lat_{t-1} \\ -\dot{Lat}_{t-1} \\ -\dot{Lon}_{t-1}\sin Lat_{t-1} \end{bmatrix} \tag{13}$$

In (10), $\mathbf{g}_{t-1}^n$ is the gravitational acceleration vector, and the time difference of the quaternion is first calculated as follows to calculate $\boldsymbol{\omega}_{nb,t}^b$.

$$d\mathbf{Qtn}_t \equiv \begin{bmatrix} dq_{(1),t} & dq_{(2),t} & dq_{(3),t} & dq_{(4),t} \end{bmatrix}^T$$
$$= \mathbf{Qtn}_{t-1}^{CT} * \mathbf{Qtn}_t \tag{14}$$

where $\mathbf{Qtn}$ is the quaternion, and superscript CT means conjugate transpose.

If $dq_{(1),t}$ is 1, $\boldsymbol{\omega}_{nb,t}^b$ is $\begin{bmatrix} 0 & 0 & 0 \end{bmatrix}^T$. Otherwise, $\boldsymbol{\omega}_{nb,t}^b$ is calculated as

$$\boldsymbol{\omega}_{nb,t}^b = \left(dq_{(2:4),t}/\sqrt{1 - dq_{(1),t}^2} \right)(2\cos^{-1} dq_{(1),t}/\Delta t) \tag{15}$$

The errors are added to the IMU data generated through (10) as follows:

$$\tilde{\mathbf{f}}_t^b = \mathbf{f}_t^b + \nabla + \mathbf{w}_{a,t}$$
$$\boldsymbol{\omega}_{ib,t}^b = \boldsymbol{\omega}_{ib,t}^b + \boldsymbol{\varepsilon} + \mathbf{w}_{g,t} \tag{16}$$

where $\nabla = \begin{bmatrix} \nabla_x & \nabla_y & \nabla_z \end{bmatrix}^T$ and $\mathbf{w}_{a,t}$ are the bias and noise of the accelerometer, and $\boldsymbol{\varepsilon} = \begin{bmatrix} \varepsilon_x & \varepsilon_y & \varepsilon_z \end{bmatrix}^T$ and $\mathbf{w}_{g,t}$ are the bias and noise of the gyro.

GPS data is generated by extracting the reference position at 1 second intervals and then errors are added. The errors are generated using Matlab Toolbox.

III. CKF-BASED INTEGRATED NAVIGATION SYSTEM DESIGN

In this article, we construct an integrated navigation system using CKF. The reason is that CKF has better performance and stability than EKF (Extended Kalman Filter) and UKF (Unscented Kalman Filter) [23]–[26]. First, the state variables are set as follows:

$$\mathbf{x} = \begin{bmatrix} \mathbf{Pos} & \mathbf{Vel}^n & \mathbf{Att} & \nabla & \boldsymbol{\varepsilon} \end{bmatrix}^T \tag{17}$$

The initial value of the navigation information is set by adding an error to the initial value of the reference trajectory, and then the state error covariance matrix is initialized in consideration of the spec of the added error. Considering the 3rd CKF, cubature points are created as follows [23]:

$$\boldsymbol{\xi}_t(i) = \hat{\mathbf{x}}_t \pm \mathbf{S}_t\sqrt{N}[1]_i \tag{18}$$

where $\boldsymbol{\xi}_t(i)$ is the ith cubature point set, $N = 15$ is system dimension, $[1]_i$ is the ith column in the unit matrix of size $N \times N$, $\mathbf{S}_t$ is calculated through Cholesky decomposition of the state error covariance matrix, and i is set to $1 \sim 2N$.

The INS algorithm is driven in synchronization with the output period of the IMU as much as the number of sets of cubature points. Through this, time propagation of the cubature points is carried out.

$$\boldsymbol{\xi}_{t+1}^-(i) = f\left(\boldsymbol{\xi}_t^-(i)\right) \tag{19}$$

where $f()$ is the INS equation [27], and superscript '-' means time propagation.

When GPS data comes in every 1 second, the measurement update is performed as follows [23], [28]:

$$\hat{\mathbf{x}}_t = \hat{\mathbf{x}}_t^- + \mathbf{K}_t(\mathbf{z}_t - \hat{\mathbf{z}}_t^-)$$
$$\mathbf{P}_t = \mathbf{P}_t^- - \mathbf{P}_{xz,t}(\mathbf{P}_{zz,t} + \mathbf{R})^{-1}\mathbf{P}_{xz,t}^T \tag{20}$$

where

$$\hat{\mathbf{x}}_t^- = \frac{1}{2N}\sum_{i=1}^{2N}\boldsymbol{\xi}_t^-(i) \tag{21}$$

$$\mathbf{z}_t = \begin{bmatrix} \mathbf{Pos}_t^{GPS} \\ \mathbf{Vel}_t^{GPS} \end{bmatrix} \tag{22}$$

$$\hat{\mathbf{z}}_t^- = \frac{1}{2N}\sum_{i=1}^{2N}\begin{bmatrix} \mathbf{Pos}(i) \\ \mathbf{Vel}^n(i) \end{bmatrix} \tag{23}$$

$$\mathbf{P}_t^- = \frac{1}{2N}\sum_{i=1}^{2N}\left(\boldsymbol{\xi}_t^-(i) - \hat{\mathbf{x}}_t^-\right)\left(\boldsymbol{\xi}_t^-(i) - \hat{\mathbf{x}}_t^-\right)^T + \mathbf{Q} \tag{24}$$

$$\mathbf{P}_{xz,t} = \frac{1}{2N}\sum_{i=1}^{2N}\left(\boldsymbol{\xi}_t^-(i) - \hat{\mathbf{x}}_t^-\right)\left(\hat{\mathbf{z}}_t^-(i) - \hat{\mathbf{z}}_t^-\right)^T \tag{25}$$

$$\mathbf{P}_{zz,t} = \frac{1}{2N}\sum_{i=1}^{2N}\left(\hat{\mathbf{z}}_t^-(i) - \hat{\mathbf{z}}_t^-\right)\left(\hat{\mathbf{z}}_t^-(i) - \hat{\mathbf{z}}_t^-\right)^T \tag{26}$$

where $\mathbf{Q}$ and $\mathbf{R}$ are the process noise covariance matrix, and the measurement noise covariance matrix, respectively. $\mathbf{Pos}_t^{GPS}$ and $\mathbf{Vel}_t^{GPS}$ are position and velocity data acquired through the GPS receiver, and $\mathbf{Pos}(i)$ and $\mathbf{Vel}^n(i)$ are data

corresponding to the position and velocity of the ith cubature point set.

In a tunnel where GPS signals cannot be received, NHC information is used as a measurement, and (22) is changed to $\mathbf{z}_t = \mathbf{0}_{2 \times 1}$ and (23) is changed as follows:

$$\hat{\mathbf{z}}_t^- = \frac{1}{2N} \sum_{i=1}^{2N} \left[(\mathbf{C}_{b,t}^n(i))^T \mathbf{Vel}^n(i) \right]_{(2:3)} \tag{27}$$

where $\mathbf{C}_{b,t}^n(i)$ is the DCM calculated using the attitude of the ith cubature point set.

If the GPS data and NHC information are used together as a measurement, (22) and (23) are changed as follows:

$$\mathbf{z}_t = \begin{bmatrix} \mathbf{Pos}_t^{GPS} \\ \mathbf{Vel}_t^{GPS} \\ 0 \\ 0 \end{bmatrix} \tag{28}$$

$$\hat{\mathbf{z}}_t^- = \frac{1}{2N} \sum_{i=1}^{2N} \begin{bmatrix} \mathbf{Pos}(i) \\ \mathbf{Vel}^n(i) \\ \left((\mathbf{C}_{b,t}^n(i))^T \mathbf{Vel}^n(i) \right)_{(2:3)} \end{bmatrix} \tag{29}$$

The time propagation and measurement update of the state variables and the state error covariance matrix are repeatedly performed, and the position, velocity, and attitude information among the state variables are provided as navigation solution. In this article, the reliability of the navigation solution is calculated through the state error covariance matrix as follows:

$$PR_t = 3\sqrt{\mathbf{P}_{(1,1),t}R_M^2 + \mathbf{P}_{(2,2),t}R_T^2 \cos^2 Lat_t + \mathbf{P}_{(3,3),t}}$$
$$VR_t = 3\sqrt{Trace(\mathbf{P}_{(4:6),t})} \tag{30}$$

where PR and VR are reliability information of position and velocity, respectively, and the units are m and m/s, respectively. And $P_{(i,j),t}$ denotes the component of the ith row and jth column of the state error covariance matrix at time t.

These reliabilities are information corresponding to 3 sigma of position and velocity errors, respectively. These information can be provided in real time while driving the navigation filter. However, whether this information properly reflects the reliability of navigation solution will be explained through simulation analysis in Section V.

IV. SAFETY MARGIN CALCULATION

The conceptual diagram of the technology for calculating the safety margin between trains based on navigation solution and reliability proposed in this study is shown in Figure 2. The safety margin calculated here is as follows:

$$SM_t = \left| \mathbf{P\hat{o}s}_{P,t} - \mathbf{P\hat{o}s}_{F,t} \right| - L_P + D_{C,t} - PR_{P,t} - PR_{F,t}$$
$$+ BD\left(\mathbf{V\hat{e}l}_{P,t} - \mathbf{V\hat{e}l}_{F,t} \right) - BD(VR_{P,t}) - BD(VR_{F,t}) \tag{31}$$

where the subscript P and F denote the preceding and following trains, respectively, and |**A**| denotes Frobenius norm of **A**. L_P is the length of the preceding train, and $D_{C,t}$ is
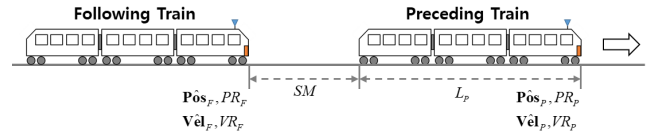

FIGURE 2. Conceptual diagram of calculating the safety margin between the preceding train and the following train.

the difference between the actual distance and the straight line distance caused by the curved trajectory between two trains. And $BD(S)$ is the braking distance by velocity S and is calculated as follows:

$$BD(S_t) = \frac{1}{2} Speed_t^2 / dec \tag{32}$$

where $Speed_t$ is the speed at the start of braking, and dec is the deceleration for braking.

Explaining (31) is as follows. The physical distance between the two trains is calculated by subtracting the length of the preceding train from the straight distance calculated by the position estimates of the two trains and then adding the additional length by the curved trajectory. However, since there is uncertainty due to the error of the position information provided by the navigation systems of the two trains, the uncertainty must be removed from the safety margin by subtracting the calculated reliability information. The safety margin calculated based on the position information corresponds to the distance between the two trains at the moment of calculation, and the braking distance by speed must be added to this so that the estimated safety margin is calculated when the trains stop. Therefore, the braking distance according to the speed difference between the two trains is added. If the speed of the preceding train is higher than that of the following train, the two trains never meet. However, in the opposite case, there is a possibility of a collision. Therefore, this term plays a very important role in calculating the safety margin. Finally, if the braking distance part according to the reliability of the velocity information provided by the navigation systems is subtracted from the previously calculated safety margin. The safety margin calculated in this way becomes the final distance information from the preceding train when the following train stops.

V. SIMULATION ANALYSIS

Simulation analysis was performed to verify the performance of the proposed technologies. The simulator developed in this study was produced based on Matlab. The technologies to be verified consist of 4 steps. The first is the generation of a reference trajectory by adding simulation conditions to the real trajectory data. The second is sensor data generation based on the reference trajectory, and the performance can be verified through the INS algorithm. The third is the reliability calculation of the navigation solution of the integrated navigation system. The performance of the reliability information according to the measurement is analyzed through comparative analysis between the state error

covariance matrix provided by the filter and RMSE through Monte Carlo simulation. And the final is the safety margin calculation based on the navigation solution and the reliability information of the integrated navigation system.

A. REFERENCE TRAJECTORY GENERATION BASED ON REAL TRAJECTORY

In order to perform the simulation of navigation technology, it is necessary to generate test trajectory. In this study, simulation was performed using real trajectory information, not virtual trajectory. As described above, by creating a reference trajectory based on the real trajectory and performing a simulation on the reference trajectory, the navigation results that can be obtained on the real trajectory were derived. For the real trajectory, the Osong test railway was selected as shown in Figure 3. This is the railway used by Korea Railroad Research Institute for testing. Since this trajectory includes straight sections, curved sections, and tunnels, it can provide various environmental information suitable for verifying the performance of the integrated navigation system.
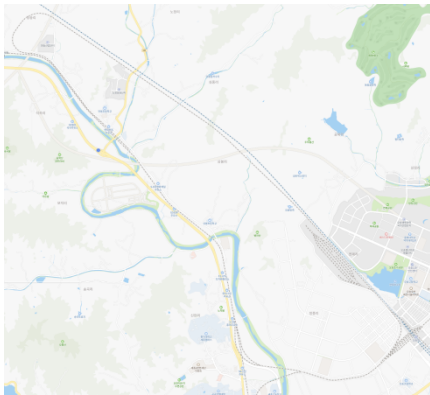

FIGURE 3. Osong test railway on the map.

First, trajectory information was acquired through the actual vehicle test. The train was equipped with an accurate trajectory acquisition equipment and operated on the test track. Through this, information such as position, velocity, attitude, GPS signal, etc. was acquired. The acquired trajectory information does not include the simulation conditions to be used in this study. Therefore, the reference trajectory was generated by adding the following simulation conditions to the acquired trajectory information: Δt of (2) was set to 0.01 sec, a_x of (4) was set to $\pm 0.44 \ m/s^2$, and the maximum speed of the train was set to 120 km/hr.

During the initial 3 minutes of the simulation, the train remains stationary on the platform, and the integrated navigation system performs initial fine alignment with zero-velocity information [29], [30]. After that, the train leaves the platform for 15 seconds. At this time, only pure INS is driven for navigation. After that, the train accelerates until it reaches its maximum speed and then moves at constant speed. At this time, the measurement update is performed in the integration filter according to the GPS signal reception condition.
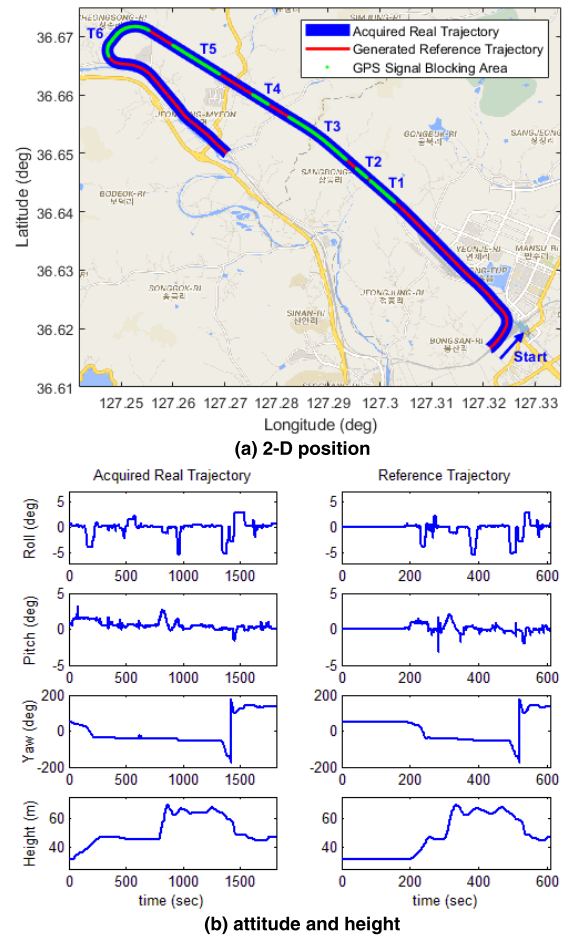

FIGURE 4. Generated reference trajectory.

And NHC information is used to perform the measurement update according to the filter selection.

Figure 4 shows the reference trajectory generated through part A of Section II. It can be seen that the generated reference trajectory exactly matches the real trajectory. Although it is not temporally synchronized with the acquired trajectory data, it can be seen that the attitude and height information calculated from the reference trajectory properly reflect the measured data. Therefore, it is verified that the accurate reference trajectory can be generated by adding the simulation conditions to the real trajectory. And it can be seen that there are 6 tunnels from T1 to T6 based on the actual GPS data. Based on this, tunnel information is added to the reference trajectory and reflected in the generation of GPS data.

B. REFERENCE TRAJECTORY-BASED IMU DATA GENERATION

IMU data was generated based on the reference trajectory through Part B of Section III. Figure 5 shows the result of processing by the INS algorithm after generating IMU data with an output frequency of 100 Hz without including sensor errors. As shown in this figure, it can be seen that the result of driving the INS algorithm using the generated

TABLE 1. Specifications of novatel's OEM-IMU-EG320N.

Sensor	Error	Spec
Gyro	bias repeatability	0.5 deg/sec
	angular random walk	0.1 deg/√hr
Accelerometer	bias repeatability	15 mg
	velocity random walk	0.05 m/s/√hr

IMU data is the same as the reference trajectory. It can be seen that complete IMU data without errors can be generated based on the reference trajectory. Real IMU data was created by including the errors in this data. The target IMU is NovAtel's OEM-IMU-EG320N, and the specifications are shown in Table 1. This IMU is a MEMS type, and one of the candidate IMUs that Korea Railroad Research Institute is considering for the development of a navigation system for trains.

C. RELIABILITY OF THE INTEGRATED NAVIGATION SYSTEM

A reference trajectory was generated based on the real trajectory, and sensor data was generated based on the reference trajectory. Using the generated reference trajectory and sensor data, it became possible to perform a simulation of the integrated navigation system. What we want to analyze in this part is the reliability of navigation information provided by the integrated navigation system. In general, the state error covariance matrix provided by the filter can be said to represent the reliability of the corresponding navigation information. However, it is necessary to check whether the environmental factors generated in the actual driving are properly reflected in this covariance matrix. To this end, we compared the state error covariance information according to the measurement and the RMSE calculated through Monte Carlo simulation. A total of 30 Monte Carlo simulations were performed. In addition, three types of integrated navigation systems were set according to the types of measurements.

- INS/GPS: In the open sky environment, measurement update is performed using GPS position and velocity information, and only pure INS is driven in the tunnel.
- INS/GPS/NHC-Option: In the open sky environment, it is the same as INS/GPS, and the measurement update is performed using NHC information in the tunnel.
- INS/GPS/NHC-Default: In the open sky environment, GPS and NHC information are used together, and in the tunnel, only NHC information is used for measurement update.

Figure 6(a) shows the RMSE of the state variables corresponding to the navigation information when only GPS measurements are used, and the standard deviation (std.) calculated through the state error covariance matrix. From this figure, it can be seen that the state error std. values appear to be smaller than RMSE in specific parts. Figure 6(b) shows the north-direction position estimation errors. Green lines are the results of Monte Carlo simulation 1 to 29, and the red
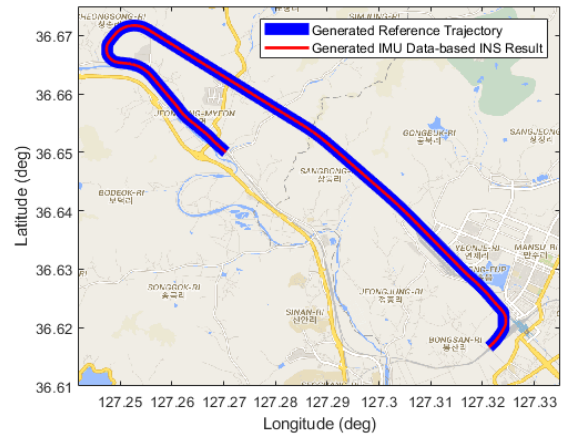

FIGURE 5. INS results using generated IMU data.

(a) RMSE vs. std.

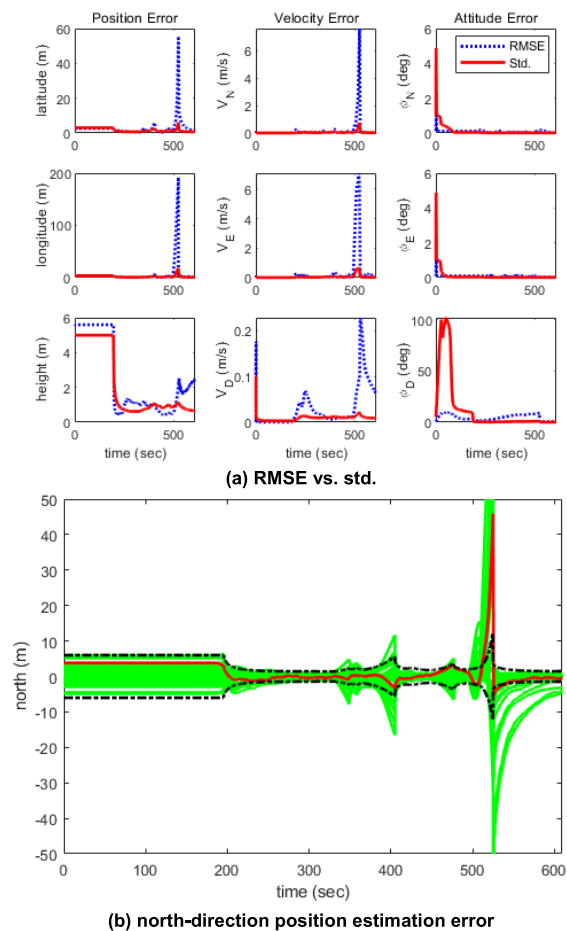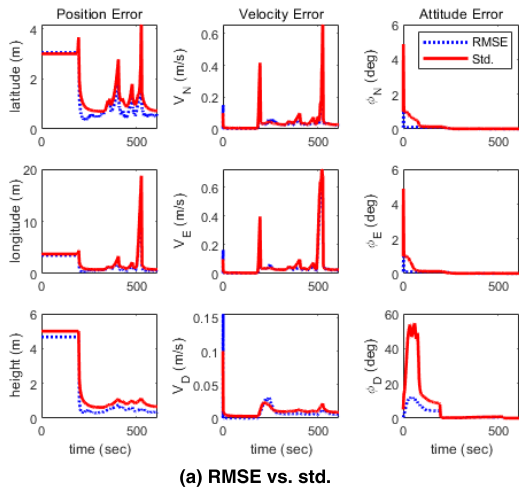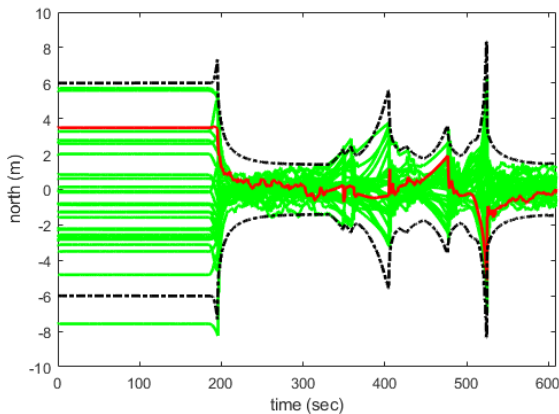(b) north-direction position estimation error

FIGURE 6. RMSE vs. state error standard deviation (INS/GPS).

line is the final simulation result. In addition, the dashed-dotted line is twice the state error std. and indicates a value of 2σ (95.4%). During the initial alignment, the covariance remains constant, and then the std. values gradually decrease through the filter update using GPS measurements as it moves. However, large and small std. increases occur in several sections. It can be seen that these sections are
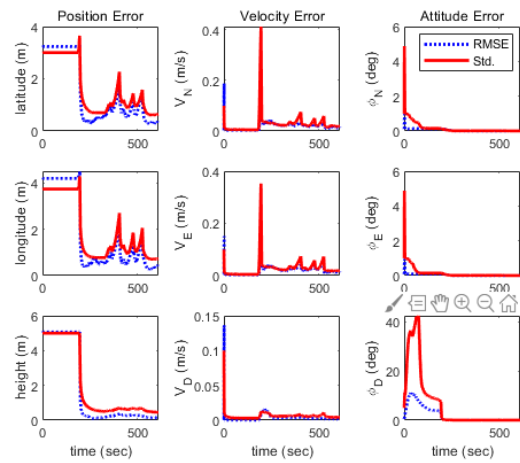
(a) RMSE vs. std.

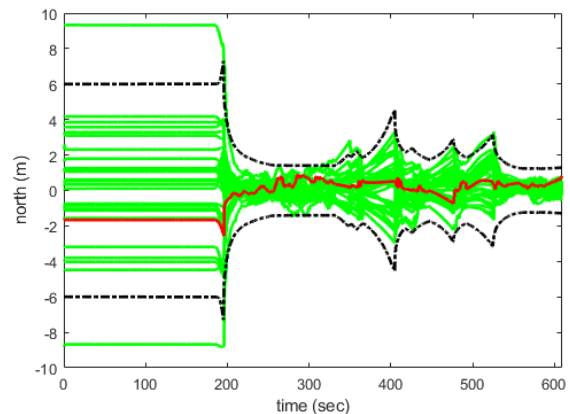(b) north-direction position estimation error

FIGURE 7. RMSE vs. state error standard deviation (INS/GPS/NHC-Option).

(a) RMSE vs. std.

(b) north-direction position estimation error

FIGURE 8. RMSE vs. state error standard deviation (INS/GPS/NHC-Default).

tunnel sections corresponding to green in Figure 4(a). In this section, the error gradually increases due to uncompensated sensor biases by calculating the position with only INS. In particular, it can be seen that the errors are greatly increased in the 3rd tunnel with a long distance and the 6th tunnel where rotation occurs within the tunnel. In these sections, the state error covariance matrix of the filter reflects the increase in the estimation error as time propagates. However, as shown in Figure 6(a), the state error std. appears to be smaller than RMSE. That is, the state error covariance matrix of the filter does not accurately reflect errors that may occur in real situation. Based on this result, it can be concluded that when an integrated navigation system is constructed using only GPS measurements, the reliability of navigation solution cannot be accurately determined only by the error covariance matrix that can be obtained in real time.

The result of the filter using the GPS/NHC-Option measurements is then shown in Figure 7. From this figure, it can be seen that the errors increase in the tunnel section, but increases within the range of the state error std. reflecting this phenomenon. And it can be confirmed that the state error std. information provided in real time has a value similar to the RMSE calculated in Monte Carlo simulation. The reason that

the azimuth error std. increases during the initial alignment process is that the azimuth error increases gradually because the observability of the z-axis gyro bias in this section is low. However, this problem is solved by updating the filter using GPS measurements while driving in open sky, so it does not affect the overall navigation.

Finally, the results of the filter using GPS/NHC-Default measurements are analyzed in Figure 8. The state error std. information calculated in real time has a similar value to the RMSE calculated in Monte Carlo simulation. This result shows similar characteristics to the case of using the GPS/NHC-Option measurements. However, comparing Figures 7 and 8, it can be seen that the position and velocity estimation errors in the tunnel sections appear much smaller when using the GPS/NHC-Option measurements. The reason is that, by always using NHC information as a measurement, it creates better navigation information than using only GPS measurements on Open Sky. Figure 9 shows the navigation errors in this case. The observability of each state variable according to the trajectory can be analyzed. It can be seen that the position information can be provided with an accuracy within $7.5m$ (2σ) even in the tunnel sections in the Osong test railway. Accuracy is also important, but in this study it is
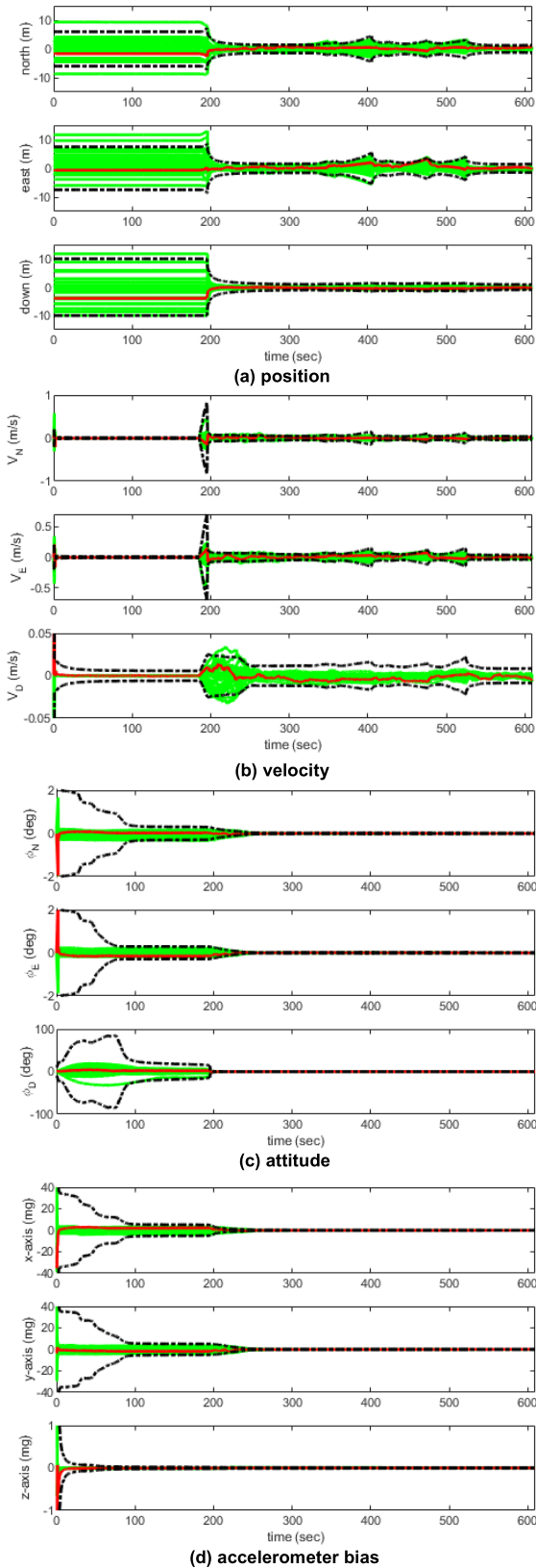
(a) position

(b) velocity

(c) attitude

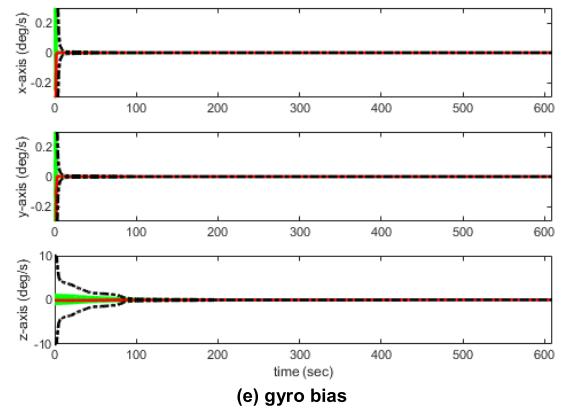(d) accelerometer bias

(e) gyro bias

FIGURE 9. *(Continued.)* State estimation errors.

more important to accurately reflect the accuracy in the state error covariance matrix.

In conclusion, it can be seen that in the case of INS/GPS/NHC-Option and INS/GPS/NHC-Default, the state error std. information provided by the real-time navigation filter reflects the reliability of navigation information well. It can also be seen that in the case of INS/GPS/NHC-Default, more accurate navigation results are estimated than in the case of INS/GPS/NHC-Option. Therefore, in this study, the integrated navigation filter is driven using the GPS/NHC-Default measurements, and based on this, the safety margin information of the train is calculated.

D. RELIABILITY INFORMATION-BASED SAFETY MARGIN CALCULATION

Figure 10 shows the simulation results of the safety margin calculated based on the navigation solution and reliability information provided by the INS/GPS/NHC integrated navigation system. It is assumed that the preceding train is stopped at the place indicated by the red triangle in Figure 10(a), and is at a position corresponding to 500 seconds after departure of the following train. The length of the preceding train was set to $226m$, and there was no error in the position and velocity information of the preceding train. And D_C in (24) was set to 0 under the assumption that map information cannot be used. $BD\left(\left|\mathbf{V}\hat{\mathbf{el}}_P - \mathbf{V}\hat{\mathbf{el}}_F\right|\right)$ and PR_F in (24) are shown in Figure 10(b). PR_F is a value calculated through the state error covariance matrix, and $BD(d\mathbf{V}\hat{\mathbf{el}})$ is calculated as (25) considering the current speed and deceleration. The deceleration was set to 0.44 m/s^2.

A simulation was performed based on a scenario in which a safety margin threshold of $1km$ was set and an alarm was provided based on the calculated safety margin. The position that provides the alarm is shown in Figure 10(c). In this figure, there is a difference between the actual distance from the preceding train and the LoS (Line-of-Sight) distance. This is
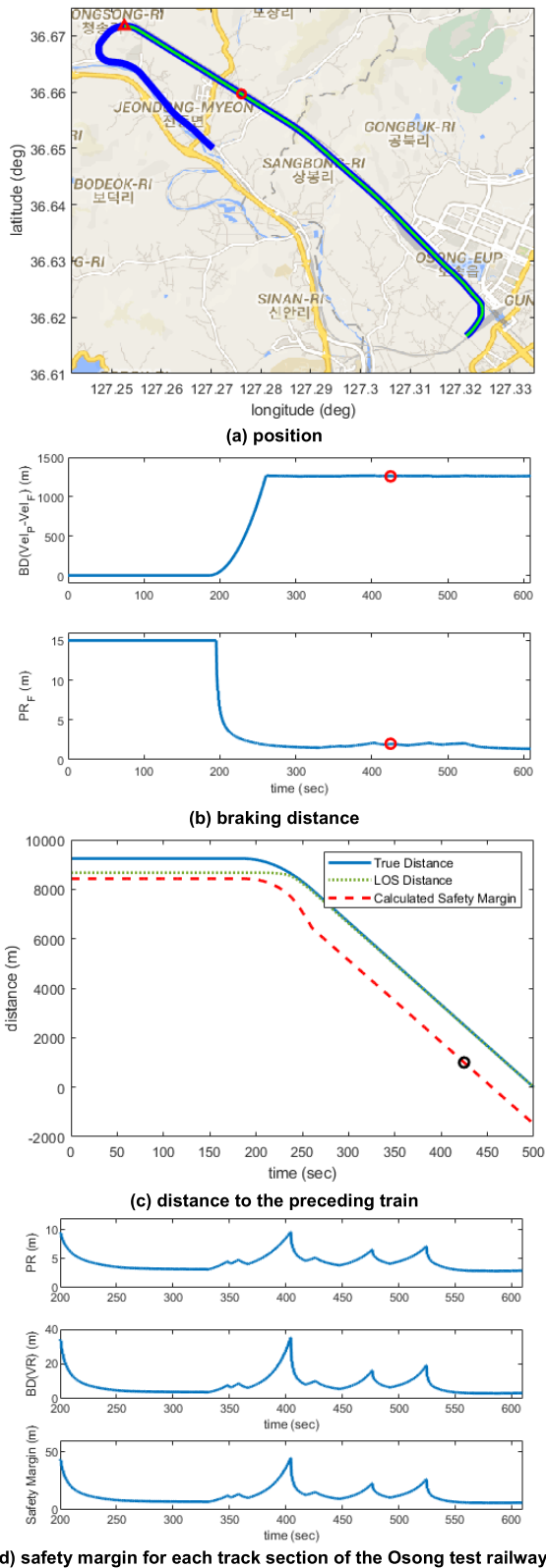
(a) position

(b) braking distance

(c) distance to the preceding train

(d) safety margin for each track section of the Osong test railway

FIGURE 10. Safety margin calculation result.

because there is a large rotational section when starting, and D_C is set to 0. This problem will have to be compensated later through map information. Going to the straight section,

the difference between these two distances decreases to a value close to zero. In this figure, the safety margin gradually decreases as the distance from the preceding train gets closer as the train speeds up, and an alarm occurs at 420 seconds, corresponding to the red circle in Figure 10(a). At this time, the actual distance from the preceding train is about 2,500m. The braking distance according to the speed information at this time is 1,259m, and considering that the length of the preceding train is 226m, it stops at 1,015m behind the preceding train after braking. Considering the reliability of the navigation solution, the train stops near the safety margin threshold set in the simulation. Therefore, it can be confirmed that the safety margin can be properly calculated through the navigation solution provided by the integrated navigation system and the reliability information of the navigation solution.

Figure 10(d) shows the safety margin calculated for each line section in the Osong test railway. The first figure shows PR_F in (24), and the second figure shows $BD(VR_F)$ calculated through (25). The errors increase in the tunnel sections, and when considering the deceleration of 0.44 m/s^2 at the current speed, it can be seen that the safety margin caused by the velocity error is larger than that caused by the position error. That is, it can be seen that the reliability of the velocity solution is more important than the reliability of the position solution. The third figure is a combination of these two information, and it is confirmed that the error of the safety margin of up to 45m in the third tunnel should be considered.

VI. CONCLUSION

In this article, a method of constructing a navigation system for trains and calculating the safety margin between trains based on this was proposed, and simulation was performed based on real trajectory information for performance verification. The contributions of this article are as follows: creating a reference trajectory by adding simulation conditions to the measured real trajectory data; generating sensor data based on the reference trajectory; analyzing the reliability of the navigation system according to the measurements and suggesting an INS/GPS/NHC integrated navigation system for trains based on this; and, the proposal of a technique to calculate the safety margin between trains based on the navigation information and the reliability information that can be provided in real time, and the simulation analysis based on the real trajectory information.

Through this article, it is possible to perform simulation based on real trajectory rather than virtual trajectory. In addition, it was confirmed that the accuracy of the navigation solution of the train is high through the integrated navigation system that always uses the NHC motion information of the train with INS/GPS, and the reliability information of the navigation solution calculated through the state error covariance matrix is excellent. Through a simulation performed based on the Osong test railway information, also, it was proved that it is possible to calculate a safety margin by using the navigation solution and the reliability information and to provide an

alarm function for maintaining a safe distance between trains even in the absence of infrastructure.

REFERENCES

[1] C. F. Lin, *Modern Navigation, Guidance, and Control Processing*. Upper Saddle River, NJ, USA: Prentice-Hall, 1991.

[2] J. Xu, G. Yang, Y. Sun, and S. Picek, "A multi-sensor information fusion method based on factor graph for integrated navigation system," *IEEE Access*, vol. 9, pp. 12044–12054, 2021.

[3] L. L. Presti, and S. Sabina, *GNSS for Rail Transportation*. Cham, Switzerland: Springer, 2018.

[4] J. Marais, J. Beugin, and M. Berbineau, "A survey of GNSS-based research and developments for the European railway signaling," *IEEE Trans. Intell. Transport. Syst.*, vol. 18, no. 10, pp. 2602–2618, Oct. 2017.

[5] K. Kim, S. Seol, and S.-H. Kong, "High-speed train navigation system based on multi-sensor data fusion and map matching algorithm," *Int. J. Control, Autom. Syst.*, vol. 13, no. 3, pp. 503–512, Jun. 2015.

[6] A. Mirabadi, F. Schmid, and N. Mort, "Multisensor integration methods in the development of a fault-tolerant train navigation system," *J. Navigat.*, vol. 56, no. 3, pp. 385–398, Sep. 2003.

[7] H. Zhang, J. Rong, and X. Zhong, "Research of the INS/GPS integrated navigation system for high speed trains," in *Proc. 9th Int. Conf. Young Comput. Sci.*, Nov. 2008, pp. 1659–1663.

[8] J. Liu, B.-G. Cai, Y.-P. Wang, J. Wang, and W. Shangguan, "A GPS/compass based train integrated positioning method for high-speed railways," in *Proc. IEEE-APS Topical Conf. Antennas Propag. Wireless Commun. (APWC)*, Sep. 2012, pp. 1201–1204.

[9] C. Legrand, J. Beugin, E. M. El-Koursi, J. Marais, M. Berbineau, and B. Conrard, "Approach for evaluating the safety of a satellite-based train localization system through the extended integrity concept," in *Proc. Eur. Saf. Rel. Conf.* Zurich, Switzerland, Sep. 2015.

[10] J. Jang and C. Kee, "Flight test of attitude determination system using multiple GPS antennae," *J. Navigat.*, vol. 59, no. 1, pp. 119–133, Jan. 2006.

[11] S. Y. Cho, "Development of an IGVM integrated navigation system for vehicular lane-level guidance services," *J. Positioning, Navigat., Timing*, vol. 5, no. 3, pp. 119–129, Sep. 2016.

[12] W. J. Park, J. W. Song, C. H. Kang, J. H. Lee, M. H. Seo, S. Y. Park, J. Y. Yeo, and C. G. Park, "MEMS 3D DR/GPS integrated system for land vehicle application robust to GPS outages," *IEEE Access*, vol. 7, pp. 73336–73348, 2019.

[13] J. A. Farrell, and M. Barth, *The Global Positioning System & Inertial Navigation*. New York, NY, USA: McGraw-Hill, 1999.

[14] K. Kim, S.-H. Kong, and S.-Y. Jeon, "Slip and slide detection and adaptive information sharing algorithms for high-speed train navigation systems," *IEEE Trans. Intell. Transport. Syst.*, vol. 16, no. 6, pp. 3193–3203, Dec. 2015.

[15] S. S. Saab, "A map matching approach for train positioning. I. Development and analysis," *IEEE Trans. Veh. Technol.*, vol. 49, no. 2, pp. 467–475, Mar. 2000.

[16] S. S. Saab, "A map matching approach for train positioning. II. Application and experimentation," *IEEE Trans. Veh. Technol.*, vol. 49, no. 2, pp. 476–484, Mar. 2000.

[17] G. M. Siouris, *Aerospace Avionics Systems*. New York, NY, USA: Academic, 1993.

[18] D. H. Titterton, and J. L. Weston, *Strapeown Inertial Navigation Technology*. London, U.K.: Peregrinus, 1997.

[19] S. Y. Cho and B. D. Kim, "Adaptive IIR/FIR fusion filter and its application to the INS/GPS integrated system," *Automatica*, vol. 44, no. 8, pp. 2040–2047, Aug. 2008.

[20] E.-H. Shin and N. El-Sheimy, "Navigation Kalman filter design for pipeline pigging," *J. Navigat.*, vol. 58, no. 2, pp. 283–295, Apr. 2005.

[21] S. Y. Cho, B. D. Kim, Y. S. Cho, and W. S. Choi, "Multi-model switching for car navigation containing low-grade IMU and GPS receiver," *ETRI J.*, vol. 29, no. 5, pp. 688–690, Oct. 2007.

[22] X. R. Li, Z. Zhao, and X.-B. Li, "Evaluation of estimation algorithms: Credibility tests," *IEEE Trans. Syst., Man, Cybern. A, Syst. Humans*, vol. 42, no. 1, pp. 147–163, Jan. 2012.

[23] I. Arasaratnam and S. Haykin, "Cubature Kalman filter," *IEEE Trans. Autom. Control*, vol. 54, no. 6, pp. 1254–1269, May 2009.

[24] B. Xu, P. Zhang, H. Wen, and X. Wu, "Stochastic stability and performance analysis of cubature Kalman filter," *Neurocomputing*, vol. 186, pp. 218–227, Apr. 2016.

[25] K. Reif, S. Gunther, E. Yaz, and R. Unbehauen, "Stochastic stability of the discrete-time extended Kalman filter," *IEEE Trans. Autom. Control*, vol. 44, no. 4, pp. 714–728, Apr. 1999.

[26] M. Enkhtur, "Modified unscented Kalman filter for a multirate INS/GPS integrated navigation system," *ETRI J.*, vol. 35, no. 5, pp. 943–946, Oct. 2013.

[27] J. W. Seo, H. K. Lee, G. I. Jee, and C. G. Park, "Lever arm compensation for GPS/INS/odometer integrated navigation," *Int. J. Control Autom. Syst.*, vol. 4, no. 2, pp. 247–254, Apr. 2006.

[28] S. Y. Cho, H. J. Ju, C. G. Park, H. Cho, and J. Whang, "Simplified cubature Kalman filter for reducing the computational burden and its application to the shipboard INS transfer alignment," *J. Positioning, Navigat., Timing*, vol. 6, no. 4, pp. 167–179, Dec. 2017.

[29] J. C. Fang and D. J. Wan, "A fast initial alignment method for strapdown inertial navigation system on stationary base," *IEEE Trans. Aerosp. Electron. Syst.*, vol. 32, no. 4, pp. 1501–1504, Oct. 1996.

[30] S. Y. Cho, H. K. Lee, and H. K. Lee, "Observability and estimation error analysis of the initial fine alignment filter for nonleveling strapdown inertial navigation system," *J. Dyn. Syst., Meas., Control*, vol. 135, no. 2, Mar. 2013, Art. no. 021005.

SEONG YUN CHO received the B.S., M.S., and Ph.D. degrees in control and instrumentation engineering from Kwangwoon University, Seoul, South Korea, in 1998, 2000, and 2004, respectively. From 2003 to 2004, he was an Assistant Researcher with Automation and System Research Institute, Seoul National University. He was a BK21 Post-Doctoral Fellow with Seoul National University in 2004. From 2004 to 2013, he was a Senior Researcher with the Electronics and Telecommunications Research Institute. From 2008 to 2013, he was an Adjunct Professor with the University of Science and Technology. In 2013, he joined the faculty with the Department of Robotics Engineering, Kyungil University, Gyeongsan, South Korea, where he is currently an Associate Professor. His current research topics include integrated navigation systems, pedestrian inertial navigation, wireless positioning, filtering theory for linear/nonlinear systems, sensor-based motion detection, and location-based services.

MYEONG SEOK CHAE received the B.S. degree in mechanical automotive engineering from Kyungil University, Gyeongsan, South Korea, in 2020, where he is currently pursuing the master's degree with the Department of IT Engineering. His current research topics include vehicular navigation system, pedestrian inertial navigation, and estimation theory.

KYUNG HO SHIN received the B.S. and M.S. degrees in control and instrumentation engineering from Kwangwoon University, Seoul, South Korea, in 1998 and 2000, respectively. In 2005, he joined as a Researcher with the Korea Railroad Research Institute, where he is currently a Principal Researcher. His current research topics include railway signaling, train control, RAMS, and global navigation satellite system.

● ● ●